



Synthesis and characterization of barium-doped TiO₂ nanocrystals for photocatalytic degradation of Acid Red 18 under solar irradiation

Behzad Shahmoradi^{a,b,*}, Mohammad Amin Pordel^{a,b}, Meghdad Pirsaeheb^c, Afshin Maleki^{a,b}, Shadi Kohzadi^{a,b}, Yuxuan Gong^d, Radheshyam R. Pawar^e, Seung-Mok Lee^{e,*}, H.P. Shivaraju^f, Gordon McKay^g

^aEnvironmental Health Research Center, Kurdistan University of Medical Sciences, Sanandaj, Iran, email: bshahmoradi@muk.ac.ir

^bDepartment of Environmental Health Engineering, Faculty of Health, Kurdistan University of Medical Sciences, Sanandaj, Iran

^cResearch Center for Environmental Determinants of Health (RCEDH), Kermanshah University of Medical Sciences, Kermanshah, Iran

^dKazuo Inamori School of Engineering, Alfred University, Alfred, NY, 14802, USA

^eDepartment of Energy and Environment Convergence Technology, Catholic Kwandong University, 522 Naegok-dong, Gangneung, 210-701, Korea, email: leesm@cku.ac.kr

^fDepartment of Environmental Science, School of Life Science, J.S.S. University, Shivarathreshwara Nagara, Mysore, Karnataka, IN 570015

^gDivision of Sustainability, College of Science and Engineering, Hamad Bin Khalifa University, Education City, Qatar Foundation, Doha, Qatar

Received 2 June 2017; Accepted 7 September 2017

ABSTRACT

Addition to the aesthetic negative environmental impacts, dyes have serious negative biological and chemical effects on the environment. The aim of this study was to investigate the removal of acid red 18 from aqueous solution using novel barium oxide added to titanium oxide nanocrystals. Moreover, these doping conditions resulted in reducing the bandgap energy significantly, which in turn makes them active under sunlight illumination. The barium doped TiO₂ nanocrystals were synthesized under mild hydrothermal conditions and were characterized by XRD, FTIR, SEM, and EDS to investigate the structure and textural features of the nanocrystals. The photodegradation experiments were conducted through the influence of batch degradation parameters such as pH, illumination time, nanocrystals dosage, and initial dye concentration. The results revealed that the removal efficiency of Acid Red 18 was 98.6% under acidic conditions. Moreover, the removal efficiency increased by reducing the initial dye concentration, increasing illumination time, and nanocrystals dosage. The characterization results confirmed the high crystallinity, lack of agglomeration and excellent dispersion of the barium doped TiO₂ nanocrystals in the media. Therefore, the barium doped TiO₂ nanocrystals could be used for photodegradation of organic pollutants from the aqueous media.

Keywords: Dye; Photodegradation; Bandgap; Hydrothermal; Solar illumination; Photo catalyst

1. Introduction

Discharging colored effluents by various industries such as textile, paper, cosmetics, agricultural, plastic, and leather has caused many environmental issues [1, 2]. Among the

dyes produced, the production of azo dyes accounts for around 60–70% of the annual dye production. Most of the azo dyes are carcinogenic, harmful, and resist biodegradation due to their complex chemical structures and toxic breakdown products [3]. The discharge of wastewater containing azo dye not only caused an aesthetic problem but

*Corresponding author.

also has a toxic impact on aquatic life by reducing water transparency and the oxygen transfer rate into water, which further adversely influenced the photosynthesis by plants in the aquatic environment [4]. These dyes are highly soluble in aqueous systems due to the existence of carboxyl, sulfonate, and hydroxyl groups [5]. Azo dyes impose adverse effects on many of the conventional treatment processes due to the widespread use and low biodegradability (due to the toxic and persistent non-biodegradable groups, in particular, the azo functional group) [6,7]. Due to the strict limits established for organic compounds in industrial effluents, removing pollutants from wastewater before discharge is crucial [8,9]. Various physical, chemical, and biological methods are used to treat textile wastewaters, which are different in efficiency, economic costs, and environmental impacts [10–12]. Adsorption methods transfer pollutant from one phase to another phase very effectively but create secondary pollution. Similarly, the biological treatment methods of dye removal are not applicable to the decolorization of textile industry wastewater because dyes are highly toxic to microorganisms in the process and their resistance to biodegradation results in a low efficiency in dye removal [13,14].

Today, advanced oxidation processes (AOPs) have attracted the attention of many researchers due to the environmental compatibility and high efficiency for wastewater treatment in the textile industry [15]. AOPs are based on the production of hydroxyl free radicals with a high oxidation power that results in the conversion of organic pollutants to minerals (carbon dioxide and water). Advanced oxidation processes are divided into different methods; the use of heterogeneous photocatalysts has attracted the attention of many researchers [16]. Heterogeneous photocatalysts are solids that can accelerate photocatalytic reactions in the presence of light without their consumption. Among semiconductors used in heterogeneous reactions, the most famous are titanium dioxide, indium oxide, manganese dioxide, zinc oxide and tungsten trioxide and sulfide such as zinc sulfide and cadmium sulfide [17–20]. Among semiconductor photocatalysts, titanium dioxide has attracted more attention since it remains unchanged after the catalytic cycle [21]. Titanium dioxide is available in three phases such as anatase, rutile, and brookite; however, the anatase phase is a crystalline form of higher photocatalytic activity than the other two phases [22]. Titanium dioxide is a semiconductor with a bandgap energy of 3.23 eV and require high excitation energy. In addition to low cost, it has stability, convenient access, biocompatibility and safety, and well able to absorb visible light spectrum. To be effective, and avoid their agglomeration and quick settlement in the environment, it is crucial to tailor their structure and morphology. Therefore, dopants are used to reduce the bandgap energy and in turn, to make them photoactive in visible light so the recapturing electron-hole could be postponed. Barium doped TiO₂ microspheres are assuming to be unique in electrocatalytic behaviour because of their large surface area, the void volume inside the spheres and thick shelled structures with high stability in acidic solution [23]. Doping TiO₂ with alkaline earth Ba modifies the optical absorption properties of the oxide, which in turn may influence the photoactivity [24].

Moreover, surface modifiers are an excellent option for reducing agglomeration and are well dispersed in the media [25–27]. Dye colored effluents have been investigated using TiO₂ based photocatalysts [28–31] usually in conjunction with another process such as activated carbon [29] or biological treatment [31].

Thus, the aim of the present study deals with the synthesis and characterization of barium doped titanium dioxide nanocrystals, under mild hydrothermal conditions, in order to investigate its efficiency for the photodegradation of acid red 18 dye under simple sunlight illumination.

2. Materials and methodology

2.1. Materials

For the synthesis of nanocrystals, titanium dioxide, barium oxide, hydrochloric acid (HCl), and *n*-butylamine were used as precursors. Sodium hydroxide and HCl (0.5 N) were used for pH adjustment. All chemicals used were of laboratory grade and high purity (Merck, Germany).

A stock solution of AR18 (1000 mg/L) by dissolving 1 g dye in double distilled water which was then stored in a refrigerator to prevent concentration changes. The azo dye used was Acid Red18 (AR18), a commercial brand name (AlvanSabet Co., Iran). The amount of AR18 was measured using spectrophotometry at a wavelength of 508 nm (λ_{max}). The unknown concentration of dye was calculated and the dye removal rate was determined using Eq. (1).

$$R\% = [C_i - C_f / C_i] \times 100 \quad (1)$$

where R% is the dye removal percentage, C_i is the initial dye concentration, mg/l; and C_f is the final dye concentration, mg/l. Before running each experiment, the final solution was kept in darkness under continuous shaking for 30 min in order to achieve adsorption-desorption equilibrium. No change in the spectrophotometer was observed after this step. Therefore, this step was considered as the initial base for further readings. Each experiment was carried out at 11:30–13:30 during June–August. While carrying out each photodegradation experiment, the ambient temperature was around 35±2°C and mean luminance of the sunlight was 664±20 lux.

2.2. Hydrothermal synthesis of barium doped TiO₂

Titanium dioxide (1 mol), barium oxide in a various molar ratio (1 and 2 mol) and a fixed quantity of solvent (10 ml 1 N HCl) were added and stirred for a few minutes under laboratory conditions to obtain a homogeneous mixture. Then, 0.5 ml of *n*-butyl amine was added dropwise with mixing. After determining the pH, the mixture was poured into a Teflon lined container ($V_{\text{fl}} = 10$ ml), and sealed in a General Purpose autoclave designed and kept in an oven at 100°C for 12 h to complete the chemical reactions. After a suitable reaction time, the resulting mixture was washed with double distilled water twice to remove or detach any possible pollution. After centrifugation at 5000 (RPM) the nanocrystals produced were dried at a temperature of 40–50°C [26, 28].

2.3. Characterization of barium doped TiO_2 nanocrystals

To study the morphology and size of the barium doped TiO_2 nanocrystals, scanning electron microscopy (SEM) was used (TSCAN, Czech). In order to avoid the destruction of samples caused by the accumulation of electrons emitted, the sample surface was covered with a thin layer of gold. The coated samples were attached with adhesive and the SEM images were analyzed under a vacuum condition and voltage 20 kV. The SEM used was equipped with an EDAX detector to determine the composition of the sample. A Fourier Transform Infrared Spectrometer (FTIR) (Bruker Tensor 27, Germany) was used to study the surface chemistry and functional groups in the absorption band $400\text{--}4000\text{ cm}^{-1}$ with a resolution of 4 cm^{-1} . The nanocrystal structure was studied using X-ray diffraction (XRD) (EQUNIOX3000, Inel France), and the XRD pattern was recorded by $\text{Cu K}\alpha$ radiation with a wavelength of 1.5405 \AA in the range $2\theta = 0\text{--}90^\circ$.

3. Results and discussion

3.1. Characteristics of barium doped TiO_2 nanocrystals

The powder XRD pattern of barium oxide doped TiO_2 nanocrystals is shown in Fig. 1. As the XRD pattern indicates, the diffraction angle has changed slightly. The characteristic peaks of tetragonal anatase TiO_2 at 25.92 , 38.75 , 48.9 , and 63.67 is obvious, however, there is no TiO_2 new peak on the lattice indicating that barium oxide is dispersed [32].

Applying surfactant, for controlling morphology and crystal growth, may result in adding a new functional group on the surface of the nanocrystals fabricated [33]. Hence, Fourier transform infrared (FTIR) was used to investigate the possible change in the surface chemistry of the barium doped TiO_2 nanocrystals.

Fig. 2 shows, no visible change in the spectrum of barium doped TiO_2 compared with natural TiO_2 indicating no chemical attachment of the surface modifier used, i.e. *n*-butylamine.

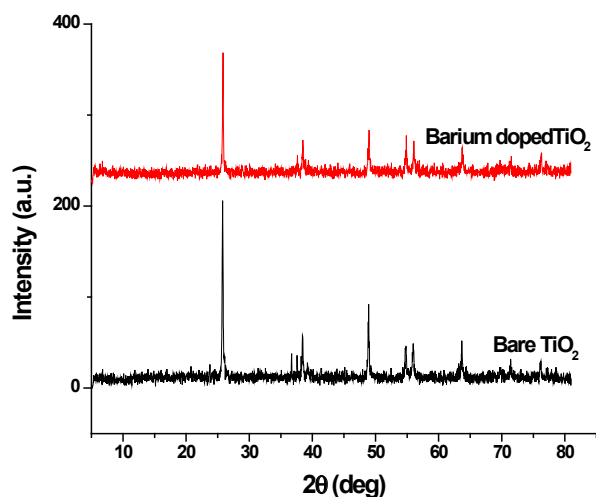


Fig. 1. Powder XRD pattern of 1 mole% barium doped TiO_2 nanocrystals.

Fig. 3 indicates, the nanocrystals have a spherical shape and less agglomeration. Such properties could be attributed to the control growth conditions imposed by the mild hydrothermal synthesis technique and the application of the surface modifier [34]. The SEM used was equipped with an EDS detector to determine the composition of the sample. The EDS scan is shown in Fig. 4.

Table 1 shows the elemental analysis of barium oxide doped TiO_2 nanocrystals. It is apparent from Table 1, that the 2% barium doped TiO_2 has carbon as an impurity, which could be attributed to an impurity in the water used for preparation of sample.

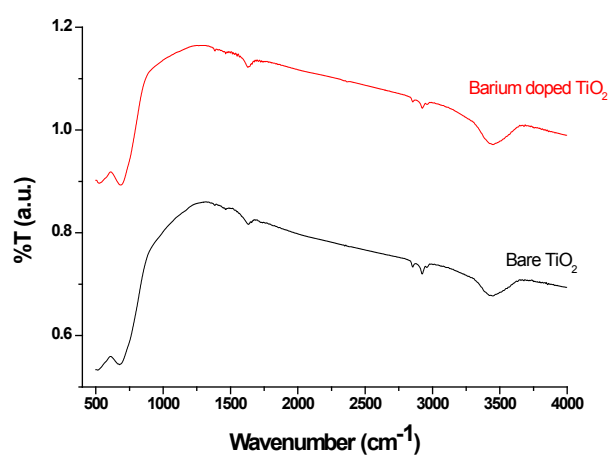


Fig. 2. FTIR spectra of 1 mole% barium doped TiO_2 nanocrystals.

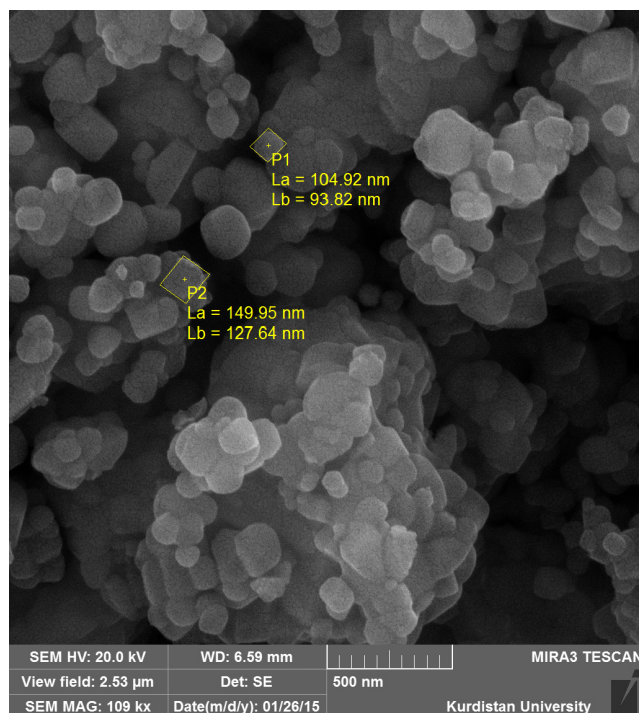


Fig. 3. Characteristic SEM of 1 mole% barium doped TiO_2 nanocrystals.

3.2. Photodegradation of AR18 using barium doped TiO₂ nanocrystals

3.1.1. Effect of molar percentage of dopant on photodegradation efficiency

Before assessing the effect of operational parameters on the photodegradation efficiency, the photodegradation of different molar types of barium doped TiO₂ were evaluated and compared with bare TiO₂. As could be expected, bare TiO₂ has negligible photodegradation efficiency under natural sunlight illumination. As depicted in Fig. 5, the photocatalytic efficiency of 1 mole% barium doped TiO₂ was higher than 2 mole% barium doped TiO₂ and significantly higher than bare TiO₂. Therefore, rest photodegradation efficiency tests were assessed using 1 mole% barium doped TiO₂ nanocrystals.

3.1.2. Effect of pH on the photodegradation of AR18

The solution pH appears to play an important role in the photocatalytic process of various pollutants [35,36]. From the stock standard solution, 25 mg/l of dye was prepared. To each sample, 2 g/l barium doped TiO₂ was added and solu-

tions of pH of 3, 7, and 11 were prepared. Later, the sample was exposed to natural sunlight illumination. An aliquot was taken in intervals of 15, 30, 45, 60, 75, and 90 min to determine the extent of dye removal using UV-Vis spectrophotometer and the removal efficiency was calculated using Eq. (1). The existence of auxochrome groups in AR18, such as hydroxyl, amino, and nitrile functional groups depending on the pH value, could justify the dye removal efficiency [37,38]. As shown in Fig. 6, under the acidic conditions (pH = 3), the removal efficiency is equal to 98.6%, while in alkaline conditions (pH = 11) is equal to 48%.

The reason for increased efficiency could be explained by the electrical zero point (pH_{zpc}) or iso-electric point of TiO₂ [39]. For TiO₂ and as determined for barium doped TiO₂, the zero point of charge (pH_{zpc}) is at pH 6.8 [40]; hence at pH < 6.8, TiO₂ surface is positively charged, and at pH values above 6.8, it is negatively charged. On this basis and given that the TiO₂ surface charge at pH lower than 6.8 is positive, the number of positive charges increases [41–43]. The increased photodegradation efficiency in acidic pH is attributed to the positively charged surface of TiO₂

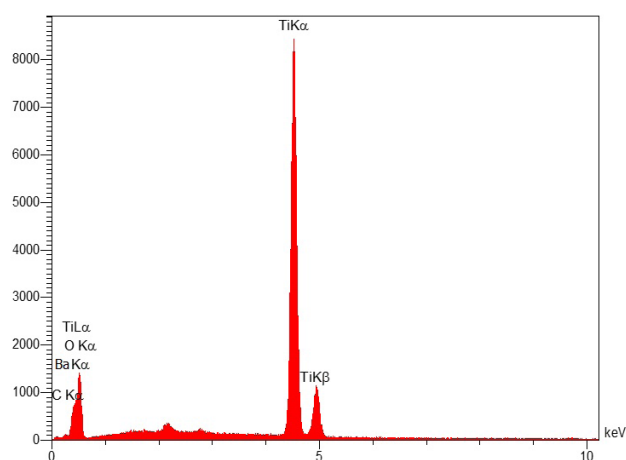


Fig. 4. Characteristic EDS of 1 mole% barium doped TiO₂ nanocrystals.

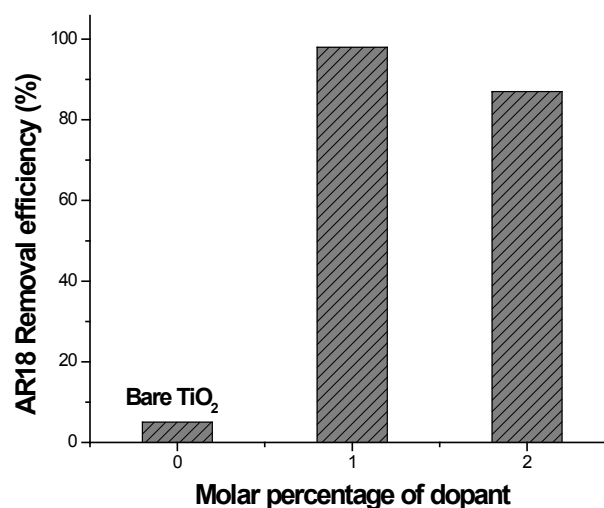


Fig. 5. Effect of dopant molar percentage on the AR18 removal efficiency.

Table 1
Elemental analysis from EDS studies of barium doped TiO₂

Compound name	Elt	Line	Int	Error	K	Kr	W%	A%	ZAF	Pk/Bg	LConf	HConf
2% Ba:TiO ₂	C	Ka	8.1	10.31	0.0043	0.0037	0.55	1.61	0.6682	2.91	0.50	0.60
	Ba	Ka	41.4	10.31	0.0341	0.0289	3.18	7.96	0.9095	8.28	3.05	3.31
	O	Ka	118.4	10.31	0.0371	0.0314	13.67	29.96	0.2300	29.58	13.34	13.9
	Ti	Ka	1635	2.31	0.9245	0.7841	82.60	60.47	0.9493	86.44	82.07	83.13
					1.0000	0.8482	100.0	100.0				
1% Ba:TiO ₂	Ba	Ka	81.8	8.43	0.0574	0.0474	5.13	12.15	0.9246	10.05	4.98	5.27
	O	Ka	170.0	8.43	0.0453	0.0374	15.98	33.17	0.2342	32.27	15.67	16.30
	Ti	Ka	1863	1.954	0.8972	0.7409	78.89	54.68	0.9391	81.43	78.42	79.36
					1.0000	0.8257	100.0	100.0				

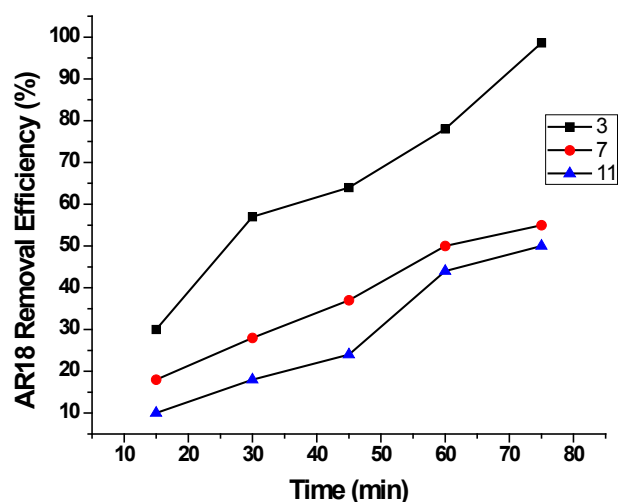


Fig. 6. Effect of pH on the photodegradation of AR18 (dye concentration = 25 mg/l; barium doped TiO₂ dosage = 2 g/l).

nanoparticles as well as the production of hydroxyl radicals, which results in an increasing photodegradation rate in acidic environment.

Moreover, the electrostatic attraction with the anionic AR18 dye results in its higher adsorption; therefore, the production of hydroxyl radicals and the degradation rate increased in an acidic environment. However, the reduced removal efficiency in an alkaline environment can be attributed to the negatively charged surface of TiO₂ nanocrystals, which results in electrostatic repulsion between the anionic AR18 and TiO₂ nanocrystals [44]. Bourikas et al. [45] found that the adsorption of acid orange 7 (AO7) by TiO₂ nanoparticles decreased as the pH increased. They reported the optimum pH was 3 for the adsorption of dye.

3.1.3. Effect of barium doped TiO₂ nanocrystals on the photodegradation of AR18

Dye samples at a concentration of 25 mg/l, pH = 3, and the nanoparticle dosage of 0.5–3.0 g/l were prepared and exposed to sunlight illumination. The samples were taken at time periods of 15, 30, 45, 60, 75, 90 min and the absorption was measured. Then the efficiency of dye removal was calculated using Eq. (1). The experiments carried out using different amounts of dye indicated that the dye removal efficiency increases with the amount of photocatalyst increasing from 0.5 to 3 g/l as shown in Fig. 7.

By increasing the amount of photocatalyst, its active surface area increases, which results in increasing bleaching efficiency. Doping TiO₂ with barium oxide increased the number of active sites on the surface of the nanocatalyst, thereby increasing the number of hydroxyl and super hydroxyl radicals, which leads to the reduction of dye removal [44,46]. The decrease in the removal efficiency of AR 18 at a higher catalyst dosage (above 2 g/L) is due to the light reflectance by catalyst particles. Similar results have been reported for the photodegradation of dyes by ZnO [47,48].

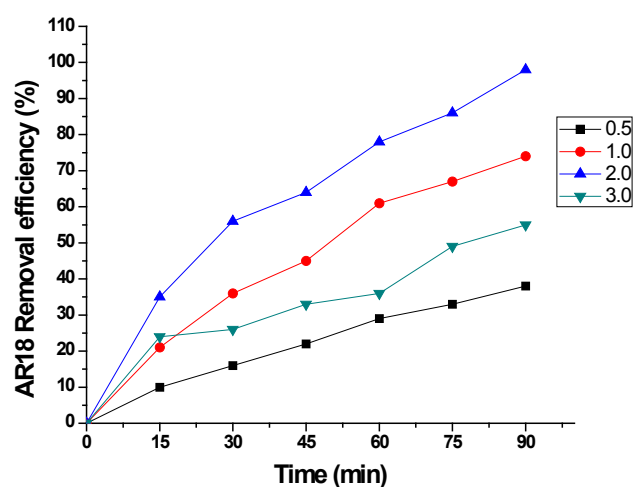


Fig. 7. Effect of barium doped TiO₂ dosage on the photodegradation of AR18.

3.1.4. Effect of the initial dye concentration on the photodegradation of AR18

The dye samples with concentrations of 25, 50, 75, and 100 mg/l, pH = 3, and the nanocatalyst dosage of 2 g/l were prepared and exposed to sunlight illumination, and at intervals of 15, 30, 45, 60, 75, and 90 min were sampled and absorption was measured. This experiment showed that the removal rate decreases with increasing concentration of dye. For the contact time of 90 min, a nanocatalyst dosage of 2 g/l, and initial dye concentration of 25 to 100 mg/l, the extent of dye removal was assessed and the removal rate decreased with increasing initial dye concentration (Fig. 8).

This suggests that removal efficiency greatly depends on the initial dye concentration, however, at higher concentrations, less catalyst surface area: dye molecules ratio is available and therefore there is less absorption and the efficiency is decreased [49]. At high concentrations of dye, reactive oxygen species in the photocatalyst surface decreases and the entry route of photons into the dye is reduced. Consequently, the number of photons on the catalyst surface decreases per number of dye molecules; hence, the absorption of photons by the catalyst decreases and the dye removal efficiency decreases [50–52]. Similar results have been reported for the photocatalytic oxidation of other dyes [53].

In all trials it has been observed that removal efficiency increases with increasing contact time. This can be attributed to providing enough time to produce active hydroxyl radicals and their subsequent occurring reactions. Moreover, the active hydroxyl radicals have sufficient time for reaction and the dye molecules degradation. In addition, reusability study of the optimized barium doped TiO₂ catalyst, was performed after each reaction cycle, by centrifugation, washing and drying at 40–50°C. The photocatalytic activity of the barium doped TiO₂ remains intact even up to third consecutive experiments under the optimized reaction conditions.

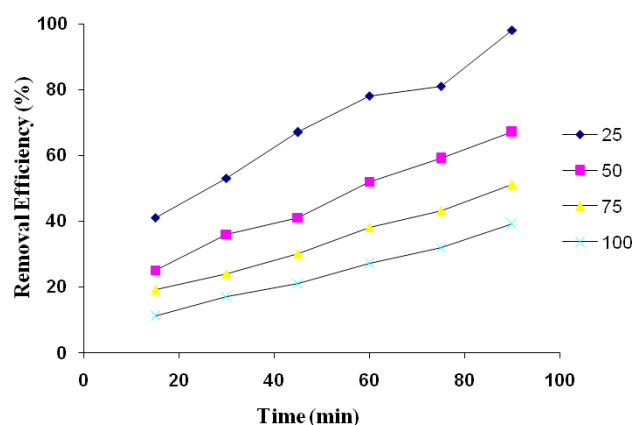


Fig. 8. Effect of the initial dye concentration on the photodegradation of AR18.

4. Conclusions

Barium doped TiO_2 nanocatalysts were successfully fabricated under mild hydrothermal conditions. The nanocatalysts fabricated were applied for degradation of acid red 18, a model dye under visible light illumination. In general, pH, nanocatalyst dosage, and the dye concentration play a very crucial role in the efficiency of the process. An increase in the amount of photocatalyst dosage, results in the increase of the dye removal because dye molecules have greater access to the surface of the nanocatalysts. In addition, the higher the dye concentration, the photodegradation efficiency decreased due to the ratio of active surface sites to the number of dye molecules decreases. Considering the excellent photodegradation efficiency, it is recommended to assess the nano-photocatalysts application for other dyes and organic pollutants.

Acknowledgement

The authors are thankful to the support provided by the Kurdistan University of Medical Sciences, Sanandaj, Iran.

References

- [1] C.-S. Lu, C.-C. Chen, F.-D. Mai, H.-K. Li, Identification of the degradation pathways of alkanolamines with TiO_2 photocatalysis, *J. Hazard Mater.*, 165 (2009) 306–316.
- [2] A.B. dos Santos, F.J. Cervantes, J.B. van Lier, Review paper on current technologies for decolourisation of textile wastewaters: Perspectives for anaerobic biotechnology, *Biores. Technol.*, 98 (2007) 2369–2385.
- [3] X. Li, T. Wang, G. Qu, D. Liang, S. Hu, Enhanced degradation of azo dye in wastewater by pulsed discharge plasma coupled with MWCNTs- $\text{TiO}_2/\gamma\text{-Al}_2\text{O}_3$ composite photocatalyst, *J. Environ. Managmt.*, 172 (2016) 186–192.
- [4] X. Quan, X. Zhang, H. Xu, In-situ formation and immobilization of biogenic nanopalladium into anaerobic granular sludge enhances azo dyes degradation, *Water Res.*, 78 (2015) 74–83.
- [5] A.R. Khataee, M.N. Pons, O. Zahraa, Photocatalytic degradation of three azo dyes using immobilized TiO_2 nanoparticles on glass plates activated by UV light irradiation: Influence of dye molecular structure, *J. Hazard. Mater.*, 168 (2009) 451–457.
- [6] A.H. Mahvi, A. Maleki, Photosonochemical degradation of phenol in water, *Desal. Wat. Treat.*, 20 (2010) 197–202.
- [7] M.L. Rache, A.R. García, H.R. Zea, A.M.T. Silva, L.M. Madeira, J.H. Ramírez, Azo-dye orange II degradation by the heterogeneous Fenton-like process using a zeolite Y-Fe catalyst—Kinetics with a model based on the Fermi's equation, *Appl. Catal. B.*, 146 (2014) 192–200.
- [8] L.S. Roselin, R. Selvin, Photocatalytic treatment and reusability of textile dyeing effluents from cotton dyeing industries, *Sci. Adv. Mater.*, 3 (2011) 113–119.
- [9] B. Pare, S.B. Jonnalagadda, H. Tomar, P. Singh, V.W. Bhagwat, ZnO assisted photocatalytic degradation of acridine orange in aqueous solution using visible irradiation, *Desalination*, 232 (2008) 80–90.
- [10] G. Al, U. Özdemir, Ö. Aksoy, Cytotoxic effects of Reactive Blue 33 on *Allium cepa* determined using Taguchi's L_8 orthogonal array, *Ecotoxicol. Environ. Safety.*, 98 (2013) 36–40.
- [11] M. Kousha, E. Daneshvar, H. Dopeikar, D. Taghavi, A. Bhatnagar, Box-Behnken design optimization of Acid Black 1 dye biosorption by different brown macroalgae, *Chem. Eng. J.*, 179 (2012) 158–168.
- [12] S. Chakraborty, B. Basak, S. Dutta, B. Bhunia, A. Dey, Decolorization and biodegradation of congo red dye by a novel white rot fungus *Alternaria alternata* CMERI F6, *Biores. Technol.*, 147 (2013) 662–666.
- [13] X. Zhou, X. Xiang, Effect of different plants on azo-dye wastewater bio-decolorization, *Procedia Environ. Sci.*, 18 (2013) 540–546.
- [14] H.-Y. Shu, C.-R. Huang, M.-C. Chang, Decolorization of mono-azo dyes in wastewater by advanced oxidation process: A case study of acid red 1 and acid yellow 23, *Chemosphere*, 29 (1994) 2597–2607.
- [15] J.J. Pignatello, E. Oliveros, A. MacKay, Advanced oxidation processes for organic contaminant destruction based on the Fenton reaction and related chemistry, *Crit. Rev. Environ. Sci. Technol.*, 36 (2006) 1–84.
- [16] U.I. Gaya, A.H. Abdullah, Heterogeneous photocatalytic degradation of organic contaminants over titanium dioxide: A review of fundamentals, progress and problems, *J. Photochem. Photobiol. C: Photochem. Rev.*, 9 (2008) 1–12.
- [17] A. Fujishima, X. Zhang, D.A. Tryk, Heterogeneous photocatalysis: From water photolysis to applications in environmental cleanup, *Int. J. Hydrogen Energy*, 32 (2007) 2664–2672.
- [18] V. Augugliaro, M. Litter, L. Palmisano, J. Soria, The combination of heterogeneous photocatalysis with chemical and physical operations: A tool for improving the photoprocess performance, *J. Photochem. Photobiol. C: Photochem. Rev.*, 7 (2006) 127–144.
- [19] P.K.J. Robertson, J.M.C. Robertson, D.W. Bahnemann, Removal of microorganisms and their chemical metabolites from water using semiconductor photocatalysis, *J. Hazard Mater.*, 211 (2012) 161–171.
- [20] A.I. Borhan, P. Samoila, V. Hulea, A.R. Jordan, M.N. Palamaru, Effect of Al^{3+} substituted zinc ferrite on photocatalytic degradation of Orange I azo dye, *J. Photochem. Photobiol. A Chem.*, 279 (2014) 17–23.
- [21] I.C. Flores, J.N. de Freitas, C. Longo, M.-A. De Paoli, H. Winnischofer, A.F. Nogueira, Dye-sensitized solar cells based on TiO_2 nanotubes and a solid-state electrolyte, *J. Photochem. Photobiol. A Chem.*, 189 (2007) 153–160.
- [22] T. Maggos, A. Plassais, J.G. Bartzis, C. Vasilakos, N. Moussopoulos, L. Bonafous, Photocatalytic degradation of NO_x in a pilot street canyon configuration using TiO_2 -mortar panels, *Environ. Monit. Assess.*, 136 (2008) 35–44.
- [23] J.E. Son, J. Chattopadhyay, D. Pak, Electrocatalytic performance of Ba-doped TiO_2 hollow spheres in water electrolysis, *Int. J. Hydrogen Energy*, 35 (2010) 420–427.
- [24] K. Vijayalakshmi, D. Sivaraj, Synergistic antibacterial activity of barium doped TiO_2 nanoclusters synthesized by microwave processing, *RSC Adv.*, 6 (2016) 9663–9671.
- [25] C.P. Sajan, B. Shahmoradi, H.P. Shivaraju, K.M.L. Rai, S. Ananda, M.B. Shayan, T. Thonthai, G.V.N. Rao, K. Byrappa, Photocatalytic degradation of textile effluent using hydrothermally

- synthesised titania supported molybdenum oxide photocatalyst, *Mater. Res. Innovat.*, 14 (2010) 89–94.
- [26] B. Shahmoradi, I.A. Ibrahim, N. Sakamoto, S. Ananda, R. Somashekar, T.N.G. Row, K. Byrappa, Photocatalytic treatment of municipal wastewater using modified neodymium doped TiO₂ hybrid nanoparticles, *J. Environ. Sci. Health Part A.*, 45 (2010) 1248–1255.
- [27] B. Shahmoradi, K. Soga, S. Ananda, R. Somashekar, K. Byrappa, Modification of neodymium-doped ZnO hybrid nanoparticles under mild hydrothermal conditions, *Nanoscale*, 2 (2010) 1160–1164.
- [28] B. Shahmoradi, M. Negahdary, A. Maleki, Hydrothermal synthesis of surface-modified, manganese-doped TiO₂ nanoparticles for photodegradation of methylene blue, *Environ. Eng. Sci.*, 29 (2012) 1032–1037.
- [29] O.K. Mahadwad, P.A. Parikh, R.V. Jasra, C. Patil, Photocatalytic degradation of reactive black-5 dye using TiO₂-impregnated activated carbon, *Environ. Technol.*, 33 (2012) 307–312.
- [30] C. Andriantsiferana, E.F. Mohamed, H. Delmas, Photocatalytic degradation of an azo-dye on TiO₂/activated carbon composite material, *Environ. Technol.*, 35 (2014) 355–363.
- [31] D. Chebli, F. Fourcade, S. Brosillon, S. Nacef, A. Amrane, Integration of photocatalysis and biological treatment for azo dye removal – application to AR183, *Environ. Technol.*, 32 (2011) 507–514.
- [32] K. Porkodi, S.D. Arokiamary, Synthesis and spectroscopic characterization of nanostructured anatase titania: A photocatalyst, *Mater. Charact.*, 58 (2007) 495–503.
- [33] K. Salehi, H. Daraei, P. Teymouri, A. Maleki, Hydrothermal synthesis of surface-modified copper oxide-doped zinc oxide nanoparticles for degradation of acid black 1: Modeling and optimization by response surface methodology, *J. Adv. Environ. Health Res.*, 2 (2014).
- [34] A. Maleki, B. Shahmoradi, Solar degradation of Direct Blue 71 using surface modified iron doped ZnO hybrid nanomaterials, *Water Sci. Technol.*, 65 (2012) 1923.
- [35] N. Sobana, M. Swaminathan, The effect of operational parameters on the photocatalytic degradation of acid red 18 by ZnO, *Sep. Purif. Technol.*, 56 (2007) 101–107.
- [36] M.S.T. Gonçalves, A.M.F. Oliveira-Campos, E.M.M.S. Pinto, P.M.S. Plasência, M.J.R.P. Queiroz, Photochemical treatment of solutions of azo dyes containing TiO₂, *Chemosphere*, 39 (1999) 781–786.
- [37] B. Subash, B. Krishnakumar, M. Swaminathan, M. Shanthi, Highly Efficient, Solar Active, and Reusable Photocatalyst: Zr-Loaded Ag–ZnO for Reactive Red 120 Dye Degradation with Synergistic Effect and Dye-Sensitized Mechanism, *Langmuir*, 29 (2013) 939–949.
- [38] A. Senthilraja, B. Krishnakumar, B. Subash, A.J.F.N. Sobral, M. Swaminathan, M. Shanthi, Sn loaded Au–ZnO photocatalyst for the degradation of AR 18 dye under UV-A light, *J. Ind. Eng. Chem.*, 33 (2016) 51–58.
- [39] Y. Luo, Y. Tian, A. Zhu, H. Liu, J. Zhou, pH-dependent electrochemical behavior of proteins with different isoelectric points on the nanostructured TiO₂ surface, *J. Electroanal. Chem.*, 642 (2010) 109–114.
- [40] N. Sobana, K. Selvam, M. Swaminathan, Optimization of photocatalytic degradation conditions of Direct Red 23 using nano-Ag doped TiO₂, *Sep. Purif. Technol.*, 62 (2008) 648–653.
- [41] M.R. Hoffmann, S.T. Martin, W. Choi, D.W. Bahnemann, Environmental Applications of Semiconductor Photocatalysis, *Chem. Rev.*, 95 (1995) 69–96.
- [42] F. Kiriakidou, D.I. Kondarides, X.E. Verykios, The effect of operational parameters and TiO₂-doping on the photocatalytic degradation of azo-dyes, *Catal. Today.*, 54 (1999) 119–130.
- [43] S. Dutta, S.A. Parsons, C. Bhattacharjee, P. Jarvis, S. Datta, S. Bandyopadhyay, Kinetic study of adsorption and photo-decolorization of Reactive Red 198 on TiO₂ surface, *Chem. Eng. J.*, 155 (2009) 674–679.
- [44] S. Garcia-Segura, S. Dosta, J.M. Guilemany, E. Brillas, Solar photoelectrocatalytic degradation of Acid Orange 7 azo dye using a highly stable TiO₂ photoanode synthesized by atmospheric plasma spray, *Appl. Catal. B Environ.*, 132 (2013) 142–150.
- [45] K. Bourikas, M. Styliidi, D.I. Kondarides, X.E. Verykios, Adsorption of Acid Orange 7 on the Surface of Titanium Dioxide, *Langmuir*, 21 (2005) 9222–9230.
- [46] M.A. Behnajady, H. Eskandarloo, Preparation of TiO₂ nanoparticles by the sol-gel method under different pH conditions and modeling of photocatalytic activity by artificial neural network, *Res. Chem. Intermed.*, 41 (2015) 2001–2017.
- [47] R. Velmurugan, B. Krishnakumar, B. Subash, M. Swaminathan, Preparation and characterization of carbon nanoparticles loaded TiO₂ and its catalytic activity driven by natural sunlight, *Sol. Energy Mater. Sol. Cells*, 108 (2013) 205–212.
- [48] Ö.E. Kartal, M. Erol, H. Oğuz, Photocatalytic destruction of phenol by TiO₂ powders, *Chem. Eng. Technol.*, 24 (2001) 645–649.
- [49] W.S. Kuo, P.H. Ho, Solar photocatalytic decolorization of methylene blue in water, *Chemosphere*, 45 (2001) 77–83.
- [50] Z. Zhang, Yuan, G. Shi, Y. Fang, L. Liang, H. Ding, L. Jin, Photoelectrocatalytic activity of highly ordered TiO₂ nanotube arrays electrode for azo dye degradation, *Environ. Sci. Technol.*, 41 (2007) 6259–6263.
- [51] D. Qu, Z. Qiang, S. Xiao, Q. Liu, Y. Lei, T. Zhou, Degradation of Reactive Black 5 in a submerged photocatalytic membrane distillation reactor with microwave electrodeless lamps as light source, *Separat. Purif. Technol.*, 122 (2014) 54–59.
- [52] A. Mills, R.H. Davies, D. Worsley, Water purification by semiconductor photocatalysis, *Chem Soc Rev.*, 22 (1993) 417–425.
- [53] I. Poullos, I. Aetopoulou, Photocatalytic degradation of the textile dye reactive orange 16 in the presence of TiO₂ suspensions, *Environ. Technol.*, 20 (1999) 479–487.